



An Approximate Model for Slug Flow Heat Transfer in Channels of Arbitrary Cross Section

M. Kalteh^{1,*}, A. Abbassi² and M. Bahrani³

¹Assistant Professor, Department of Mechanical Engineering, University of Guilan, Rasht, Iran

²Professor, Department of Mechanical Engineering, Amirkabir University of Technology, Tehran, Iran

³Associate Professor, School of Engineering Science, Simon Fraser University, B.C., Canada

Abstract

In this paper, a novel approximate solution to determine the Nusselt number for thermally developed, slug (low-Prandtl), laminar, single phase flow in channels of arbitrary cross section is presented. Using the Saint-Venant principle in torsion of beams, it is shown that the thermally developed Nusselt number for low-Prandtl flow is only a function of the geometrical parameters of the channel cross section, i.e., area, perimeter and non-dimensional polar moment of inertia. The new proposed model is compared with the existing numerical results for elliptic, rectangular, regular polygonal, flat plate, isosceles triangular, equilateral triangular and circular sector channels. The model predicts the Nusselt number for the above mentioned channels within the about 10% or better with the exception of the circular sector in very small aspect ratios. The new model is expected to be accurate for other singly connected channels and can be used to determine the fully developed turbulent Nusselt number for liquid metal flows. Finally, the proposed model is used to determine the slug flow Nusselt number for unavailable geometries in the literature such as rhombic, circular segment, annular sector channel as well as rectangular channel with semicircular ends.

Keywords: Nusselt number; Laminar; Slug; Arbitrary cross section; Approximate model.

1. Introduction

In the low-Prandtl (slug) flow, velocity profile remains constant and uniform, while the temperature profile develops. Low-Prandtl flow is an approximation for hydrodynamic entrance region of laminar fluid flows with negligible Prandtl number. On the other hand, that can be regarded as a simplified model for the analysis of turbulent flows and fully developed laminar flow of a pseudoplastic fluid with a vanishing power-law index. According to Hartnett and Irvine [1], the fully developed turbulent Nusselt number for liquid metals can be expressed as a function of the slug flow Nusselt number. To do this, knowing the slug flow Nusselt number for different channel cross sections will be valuable.

In the literature, there are some studies involving the slug flow forced convection heat transfer in ducts. Hartnett and Irvine [1] presented slug flow Nusselt numbers for some noncircular ducts and for three different boundary conditions. Also, slug flow with

viscous dissipation in circular ducts was studied analytically [2–4]. Barletta [2] studied the effect of the viscous dissipation on the fully developed Nusselt number of slug flow in circular ducts for various axial distributions of the wall heat flux. Barletta and Zanchini [3] investigated the same problem as [2] but in the thermal entrance region. Also, Barletta [4] studied the effect of the viscous dissipation on the slug flow Nusselt number in the thermal entrance region when the tube wall exchanges heat with external fluid. Gao and Hartnett [5] developed an analytical solution for rectangular channels under H2 Boundary condition and for different combinations of the heated walls using the superposition method. This problem was studied by Spiga and Morini [6] in the thermal entrance region. For three boundary conditions of T, H1 and H2 in the thermally developed region of a rectangular duct, Morini [7] developed an analytical solution using the finite-integral transform method. He presented the temperature profile and the Nusselt number on graphs and tables. The effect of the viscous dissipation on the

* Corresponding author, Phone: +98-1316690274(3078)
Email: mkalteh@guilan.ac.ir

developing Nusselt number in rectangular channels under different combinations of the H2 boundary condition, was studied analytically by Barletta and Pulvirenti [8] using the superposition method. They let the wall heat flux to vary in axial direction exponentially.

According to the literature review, the obtained results are just for simple geometries and finding an analytical solution for many practical singly-connected channels is very complex or impossible. In many engineering applications such as basic design and optimization it is just required to obtain the trends and the reasonable estimates suffices. In such circumstances, solving the governing exact equations is unfavorable. Muzychka and Yovanovich [9] introduced a geometrical mapping for predicting the fully developed Nusselt number in noncircular ducts. They mapped the noncircular ducts into equivalent rectangular channels using the appropriate definition of the aspect ratio for each channel. They proposed the use of the square root of the cross sectional area as the characteristic length instead of the hydraulic diameter and showed that the $Nu_{\sqrt{A}}$ is a weak function of the geometry of the channel cross section.

This paper aims to present an approximate model to predict the thermally developed slug flow in channels of the arbitrary cross section under the H1 boundary condition. The proposed model is compared with the existing results for channels such as: rectangular, elliptical, isosceles triangular, circular sector and regular polygonal. After successful validation of the model with these channels, the proposed model can be extended for the case of the arbitrary cross section channels such as rhombic, circular segment, annular sector channel as well as rectangular channel with semicircular ends.

2. Problem formulation

The assumptions of the proposed model are:

- Thermally developed, slug, steady state and laminar flow
- H1 boundary condition is applied on the channel boundary
- Constant cross sectional area A and constant perimeter P
- Constant fluid properties
- Negligible viscous dissipation and natural convection
- Negligible axial heat conduction in the fluid

Some researches such as Thiar [10] has stated that in the laminar flow for low Prandtl numbers, the Peclet number is very small and as a result, the axial conduction in the fluid cannot be neglected. But Nield and Lage [11] using the analytical analysis showed that for the case of the slug flow, the finite axial conduction in the fluid has no effect on the Nusselt number value. Thus, in the present study, the effect of the axial heat

conduction is neglected.

For q' as the axially uniform heat flux per unit length of the duct, the energy equation is:

$$\frac{\partial^2 T}{\partial x^2} + \frac{\partial^2 T}{\partial y^2} = \frac{q'}{\rho A c_p \alpha} \quad (1)$$

and the no-temperature jump boundary condition is applied on the channel walls:

$$T = T_w \quad (2)$$

It is clear that Eq. (1) is a Poisson equation. The proposed model is based on the analytical solution of the elliptical channel, not because it is likely to occur in practice, but rather to utilize the unique geometrical property of its velocity solution.

Now, using the variable change as $\theta = T - T_w$, Eq. (1) can be written as follows:

$$\frac{\partial^2 \theta}{\partial x^2} + \frac{\partial^2 \theta}{\partial y^2} = \frac{q'}{\rho A c_p \alpha} \quad (3)$$

and the boundary condition can be written as $\theta = 0$.

On the other hand, the fully developed momentum equation in the z direction (flow direction) can be written as:

$$\frac{\partial^2 w}{\partial x^2} + \frac{\partial^2 w}{\partial y^2} = \frac{1}{\mu} \frac{dp}{dz} = c_1 \quad (4)$$

which is supplemented by the no-slip boundary condition, i.e., $w=0$.

Inspecting the Eqs. (3) and (4) along with the boundary conditions, the analogy between the fully developed momentum equation and the slug flow energy equation is understandable. Thus, using the existing solution for fully developed velocity profile, one can obtain the developed temperature profile in slug flow. The fully developed velocity profile for an elliptical channel can be written as [12]:

$$\bar{w} = \frac{-c_1 b^2}{4(1 + \varepsilon^2)} \quad (5)$$

where ε is the aspect ratio defined as:

$$\varepsilon = \frac{b}{a} \quad (6)$$

a and b are the major and minor semi-axes of the elliptic cross section, $a \geq b$.

According to the above-mentioned analogy, the mean bulk temperature can be written as:

$$\theta_m = \frac{-q' b^2}{4\rho A c_p \alpha (1 + \varepsilon^2)} \quad (7)$$

Having the mean bulk temperature in hand, one can obtain the thermally developed Nusselt number for slug flow. Based on the hydraulic diameter:

$$Nu_{D_h} = \frac{\bar{h} D_h}{k} \quad (8)$$

In this problem, T_w is constant peripherally (H1 B.C.). It should be noted that in practice, achieving this boundary condition is difficult for non-circular channels, but since it is mathematically amenable, it is

investigated in the literature [12]. Thus, h varies along the channel perimeter and the average h must be used. Considering this issue:

$$\bar{h} = \frac{q'}{P(T_w - T_m)} \quad (9)$$

thus:

$$Nu_{D_h} = \frac{q' D_h}{P(T_w - T_m)k} \quad (10)$$

For elliptical channel, the hydraulic diameter is as follows:

$$D_h = \frac{\pi b}{E(e)} \quad (11)$$

where $E(e)$ is the complete elliptic integral of the second kind and $e = \sqrt{1 - \varepsilon^2}$.

Substituting the Eqs. (7) and (11) in Eq. (10), the Nusselt number for elliptic channel can be written as:

$$Nu_{D_h} = \frac{\pi^2(1 + \varepsilon^2)}{E^2(e)} \quad (12)$$

Similar to Muzychka and Yovanovich [9] it is likely to define the Nusselt number based on the square root of the cross sectional area to reduce the effect of the channel geometry. Thus, Eq. (12) can be written as:

$$Nu_{\sqrt{A}} = \frac{P}{4\sqrt{A}} Nu_{D_h} = \frac{\pi^2(1 + \varepsilon^2)}{E(e)\sqrt{\pi\varepsilon}} \quad (13)$$

in which for an elliptical channel:

$$\begin{cases} P = 4aE(e) \\ A = \pi ab \end{cases} \quad (14)$$

Fig. 1 shows the comparison of the obtained results using the Eq. (13) with the results of the Hartnett and Irvine [1]. The maximum percentage error is 1.19% and that is due to the errors in computing the elliptic integral $E(e)$ and reading the data from the graphs.

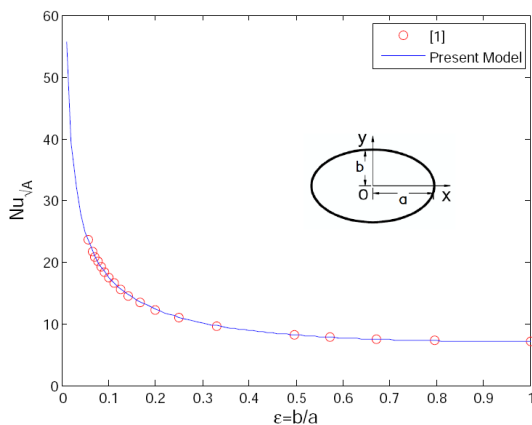


Fig. 1. Comparison between new model results and the numerical results of [1]

Torsion in beams, fully developed laminar flow in ducts and thermally developed energy equation for slug flow in channels are similar in the sense that the governing equations for all is Poisson's equation.

Therefore, similar to Bahrami et al. [13], using the Saint-Venant principle, one can use the results of the elliptical channel to predict the thermally developed Nusselt number for slug flow in noncircular ducts. Thus, it remains to write the Eq. (13) as a function of the geometric parameters. For an elliptical channel, the polar moment of inertia is:

$$I_p = \frac{\pi ab(a^2 + b^2)}{4} \quad (15)$$

Substituting Eqs. (14) and (15) in Eq. (13):

$$Nu_{\sqrt{A}} = 16\pi^2 I_p^* \frac{\sqrt{A}}{P} \quad (16)$$

in which $I_p^* = \frac{I_p}{A^2}$ is the non-dimensional polar moment of inertia.

It is expected that Eq. (16) can be used for other noncircular cross sections. On other words, for each noncircular channels it is sufficient to compute the geometric parameters (perimeter, area, polar moment of inertia) to predict the thermally developed Nusselt number for slug flow. In the next section, the model results will be compared with the existing solutions for different cross sections.

3. Results and discussions

In this section, the results of the new model (Eq. (16)) are compared with the existing solutions for various noncircular ducts and then the thermally developed slug flow Nusselt number for some other geometries that there are no data available for them in the literature are calculated. The following relationship is used to convert the Nusselt number based on D_h to \sqrt{A} :

$$Nu_{\sqrt{A}} = \frac{P}{4\sqrt{A}} Nu_{D_h} \quad (17)$$

3.1. Rectangular Channel

For rectangular channel the perimeter, area and non-dimensional polar moment of inertia can be determined from; $P = 4(a + b)$, $A = 4ab$ and $I_p^* = \frac{1 + \varepsilon^2}{12\varepsilon}$.

Using Eq. (16), $Nu_{\sqrt{A}}$ for the rectangular channel is:

$$Nu_{\sqrt{A}} = \frac{2\pi^2(1 + \varepsilon^2)}{3\sqrt{\varepsilon}(1 + \varepsilon)} \quad (18)$$

Fig. 2 shows the comparison between numerical results of [7] and the results of Eq. (18). The comparison shows that maximum difference between the numerical results and the present model is 7.51%.

3.2. Regular Polygonal Channel

The perimeter, area and polar moment of inertia for n-sided regular polygonal channel can be found from:

$$P = na, A = \frac{na^2}{4\tan(\frac{\pi}{n})} \text{ and } I_p = \frac{na^4}{96\tan(\frac{\pi}{n})} \left(1 + \frac{3}{\tan^2(\frac{\pi}{n})} \right).$$

in which n is the number of sides and "a" sits for the length of each side. Thus, $Nu_{\sqrt{A}}$ for regular polygonal channel can be written as:

$$Nu_{\sqrt{A}} = \frac{4\pi^2}{3\sqrt{ntan(\frac{\pi}{n})}} \left(\tan\left(\frac{\pi}{n}\right) + \frac{3}{\tan(\frac{\pi}{n})} \right) \quad (19)$$

The comparison between the model results and the numerical results of Asako et al. [14] has been shown in Table 1. According to the table the maximum difference between the results is 7.11%. It is necessary to note that for the case of regular polygonal channel with infinity sides (circle), the magnitude of the n is considered equal to 100, while the magnitudes greater than 100 have very small effect on the Nusslet number.

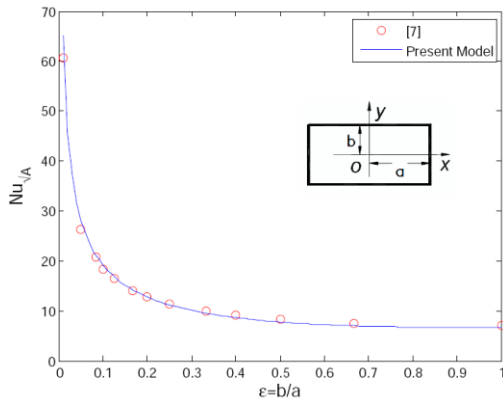


Fig. 2. Comparison between new model and the numerical results of [7]

Table 1. Percentage error between the new model and results of [14] for regular polygonal channel.

n	Nu_{\sqrt{A}}		%Diff.
	Present Model	[14]	
4	6.58	7.08	7.11
6	6.8	7.01	2.95
8	6.92	7.0	1.15
\infty(100)	7.09	7.06	0.44

3.3. Isosceles Triangular Channel

For isosceles triangular channel the relations for perimeter, area and non-dimensional polar moment of inertia are: $P = 2a + \frac{2a}{\sin\phi}$, $A=2ab$ and $I_p^* = \frac{\epsilon}{9} + \frac{1}{12\epsilon}$. Therefore, $Nu_{\sqrt{A}}$ can be written as:

$$Nu_{\sqrt{A}} = 8\pi^2 \frac{\sqrt{2\epsilon}}{(1 + \frac{1}{\sin\phi})} \left[\frac{\epsilon}{9} + \frac{1}{12\epsilon} \right] \quad (20)$$

In the above relations for isosceles triangular channel the aspect ratio relates to corner angle as $\epsilon = \frac{1}{2\tan\phi}$.

Fig. 3 shows the comparison between the model results and the numerical results of [1]. In this case the maximum error is 12.04%. For clearer comparison, Table 2 shows the percentage errors in different aspect

ratios for isosceles triangular channels. According to the table, the error increases with triangles with sharper corners.

3.4. Equilateral Triangular Channel

Equilateral triangular channel is the special case of a regular polygonal channel with n=3. For this geometry, the thermally developed slug flow Nusselt number based on the hydraulic diameter is 6.67 [1]. Also, for equilateral triangular channel the following relations are known: $\frac{\sqrt{A}}{P} = 0.219$ and $I_p^* = 0.192$. Therefore, the governing error for the model in predicting the thermally developed slug flow Nusselt number is 12.8%.

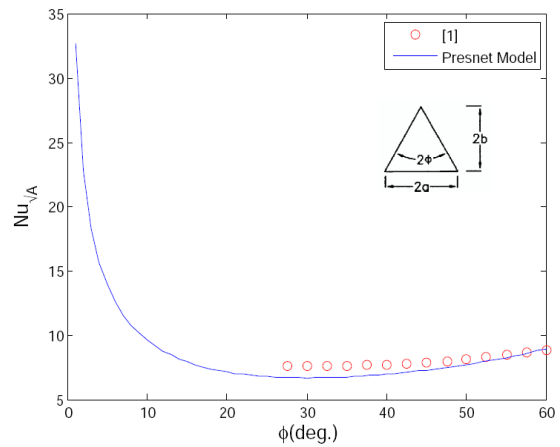


Fig. 3. Comparison between model results with results of [1] for isosceles triangular channel

3.5. Flat Plate

Flat plate can be considered as a special case of rectangular channel in which the channel aspect ratio becomes close to zero. There is an infinite series solution for flat plate in the thermal entrance region [15]. The thermally developed Nusselt number for slug flow based on the hydraulic diameter in flat plate is 12 [15].

If the flat plate is considered as a rectangular channel with aspect ratio 0.01, the model result using the Eq. (18) will have 7.5% error with respect to numerical result of [15].

3.6. Circular Sector Channel

Circular sector channel is another cross section that may be important in heat exchanger applications. For this cross section the perimeter, area and non-dimensional polar moment of inertia are: $P = 2a(1 + \phi)$, $A = a^2\phi$ and $I_p^* = \frac{9\phi^2 - 8\sin^2\phi}{18\phi^3}$. Substituting these relations in Eq. (16), one can obtain:

$$Nu_{\sqrt{A}} = \frac{4\pi^2\sqrt{\phi}}{(1 + \phi)\phi^3} (9\phi^2 - 8\sin^2\phi) \quad (21)$$

Table 2. Difference between new results and results of [1] for isosceles triangular channel.

2 ϕ (deg.)	ε	$Nu_{\sqrt{A}}$		%Diff.
		Present Model	[1]	
55.14	0.96	6.69	7.6	12.04
60.08	0.86	6.67	7.57	11.97
65.02	0.78	6.69	7.57	11.67
70.12	0.71	6.74	7.59	11.08
75.06	0.65	6.83	7.63	10.47
80	0.6	6.95	7.68	9.55
85.1	0.54	7.1	7.77	8.62
90.04	0.5	7.27	7.84	7.34
95.14	0.46	7.47	7.97	6.2
100.08	0.42	7.7	8.09	4.8
105.02	0.38	7.95	8.25	3.66
110.12	0.35	8.25	8.43	2.13
115.06	0.32	8.57	8.63	0.74
120	0.29	8.93	8.84	1.01

The results of Eq. (21) have been compared with the numerical results of [1] in Fig. 4. In this case, the percentage error for very small aspect ratios (or circular sectors with small angles) is a bit high. But, for other aspect ratios, the percentage error is smaller than 9%. For clear comparison the percentage errors are shown in Table 3 for different sector angles.

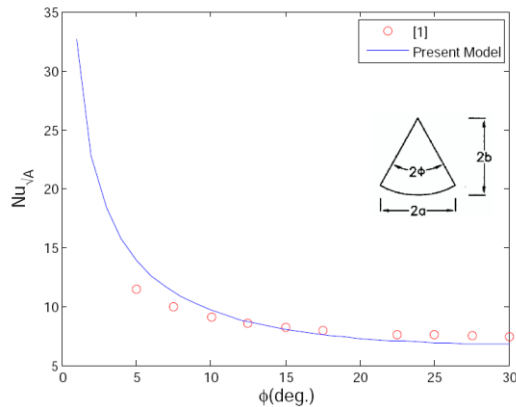


Fig. 4. Comparison Between new model results and results of [1] for circular sector channel

Table 3. Difference between new model and results of [1] for circular sector channel.

2 ϕ (deg.)	ε	$Nu_{\sqrt{A}}$		% Diff.
		Present Model	[1]	
10.03	0.17	13.91	11.45	21.56
14.96	0.26	11.23	9.91	13.24
20.05	0.35	9.65	9.05	6.61
24.99	0.43	8.68	8.54	1.71
30.08	0.52	8.02	8.16	1.81
35.01	0.6	7.57	7.94	4.59
45.04	0.77	7.05	7.63	7.58
49.97	0.84	6.91	7.54	8.37
55.07	0.92	6.83	7.47	8.63
60	1.0	6.78	7.42	8.57

3.7. Other singly-connected channels

On the above sub-sections the applicability of the new model for different channel geometries has been shown. From the results, it can be seen that the new model (eq. (16)) is able to approximately predict the thermally developed slug flow Nusselt number for above mentioned channels. So, similar to Saint-Venant principle for torsion of beams, the new model can be used to approximate the thermally developed slug flow average Nusselt number for any singly-connected channel. Therefore, this new model is applied to some of the singly-connected channels that the thermally developed slug flow Nusselt number for them is not available in the literature.

3.7.1. Rhombic Channel

Cross-sectional area, perimeter and non-dimensional polar moment of inertia for a rhombic channel with L as side of the channel, can be determined from $A = L^2 \sin\phi$, $P = 4L$ and $I_p^* = 1/(6\sin\phi)$, respectively. Fig. 5 shows the thermally developed slug flow Nusselt number for different ϕ . According to the figure, as ϕ increases, the Nusselt number decreases. On the other hand, it is clear that for $\phi=90$ the channel will be a square channel for which the Nusselt number is 6.58 from Table 1 that is exactly the same as the value in Fig. 5.

3.7.2. Circular segment channel

Cross-sectional area and perimeter for circular segment channel are calculated using the $A = a^2(\phi - 0.5\sin 2\phi)$ and $P = 2a(\phi + \sin\phi)$, respectively. Polar moment of inertia about the center of geometry is:

$$I_p = a^4 \left[\frac{\phi}{2} - \frac{\sin 2\phi(1+2\cos^2\phi)}{12} - \frac{(2\sin\phi - \cos\phi\sin 2\phi)^2}{9(\phi - 0.5\sin 2\phi)} \right]$$

Thermally developed slug flow Nusselt number for this channel at different angles is shown in Fig. 6. As can be seen from the figure, the Nusselt number approaches a constant value of 7.09 with increasing in ϕ . At the limiting case of $\phi=180$, the channel will be circular and the Nusselt number equals to the magnitude mentioned in Table 1 for $n=\infty$.

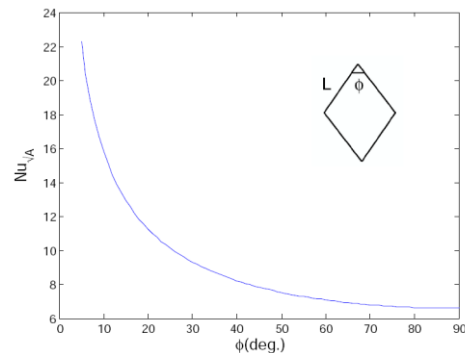


Fig. 5. New model results for thermally developed slug flow Nusselt number in a rhombic channel

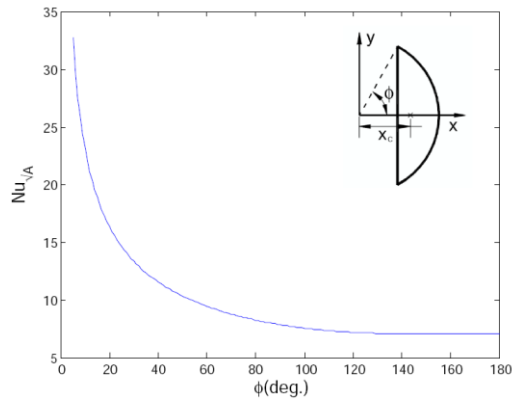


Fig. 6. New model results for thermally developed slug flow Nusselt number in a circular segment channel

3.7.3. Annular sector channel

Cross-sectional area, perimeter and non-dimensional polar moment of inertia for annular sector channel are: $A = \phi r_0^2 (1 - r^{*2})$, $P = 2r_0 [(1 + r^*)\phi + 1 - r^*]$ and $I_p^* = \frac{0.5(1-r^{*4}) - \frac{4}{9}(\frac{\sin\phi}{\phi})^2 \frac{(1-r^{*3})^2}{1-r^{*2}}}{\phi(1-r^{*2})^2}$ respectively, where $r^* = r_0/r_i$. Fig. 7 shows the new model results for this channel. According to the figure, for high values of ϕ and low r^* , the slug flow Nusselt number approaches a limiting value.

3.7.4. Rectangular channel with semicircular ends

The cross-sectional area, perimeter and polar moment of inertia for rectangular channel with semicircular ends can be calculated using: $A = a^2 [4\varepsilon(1 - \varepsilon) + \pi\varepsilon^2/2]$, $P = 2a(2 - 2\varepsilon + \pi\varepsilon)$ and

$$I_p = a^4 \left[\frac{4\varepsilon(1 - \varepsilon)[\varepsilon^2 + (1 - \varepsilon)^2]}{3} + \varepsilon^4 \left(\frac{\pi}{4} - \frac{8}{9\pi} \right) + \frac{\pi\varepsilon^2}{2} \left(1 - \varepsilon + \frac{4\varepsilon}{3\pi} \right)^2 \right]$$

respectively. The resulting thermally developed slug flow Nusselt numbers for this geometry are shown in Fig. 8 for different channel aspect ratios.

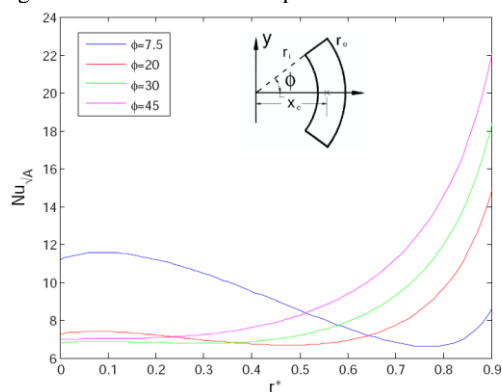


Fig. 7. New model results for thermally developed slug flow Nusselt number in an annular sector channel

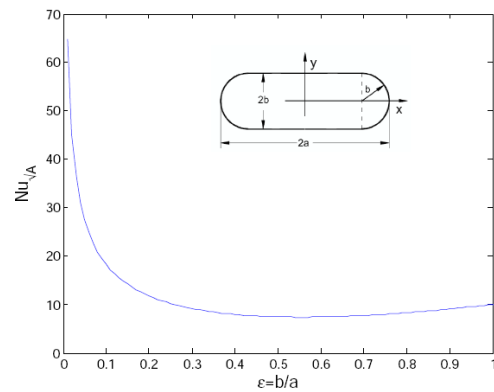


Fig. 8. New model results for thermally developed slug flow Nusselt number in a rectangular channel with semicircular ends

4. Conclusions

The slug flow forced convection heat transfer in noncircular channels is investigated. For single phase, thermally developed, laminar, steady state and slug flow in smooth channels, using the unique solution for elliptical channels and the Saint-Venant principle, a new model to predict the Nusselt number is presented. The proposed model is a function of the geometric parameters of the channel cross section. The new results of the model are compared with the existing solutions for rectangular, flat plate, regular polygonal, isosceles triangular, equilateral triangular and circular sector channels. The new results are within about 10% error or better for above channel shapes with the exception of the circular sector channel in very small aspect ratios (about smaller than 0.2). According to the obtained accuracy for above channels, it is believed that the proposed model can be extended for the general case of the singly-connected channels of the arbitrary cross section. Therefore, the model is used to determine the slug flow Nusselt number for unavailable geometries in the literature such as, rhombic, circular segment, annular sector channels as well as rectangular channel with semicircular ends. Also, the results can be used to determine the turbulent Nusselt number for liquid metals.

Nomenclature

A	cross-sectional area, m ²
a, b	dimension of the channel, m
D _h	hydraulic diameter, m
E(.)	elliptic integral of second kind
I _p	polar moment of inertia, m ⁴
I _p [*]	nondimensional polar moment of inertia
Nu	Nusselt number
n	number of polygonal channel sides
P	perimeter, m
r	radius, m
w	velocity, m/s

\bar{w} average velocity, m/s

Greek symbols

ε aspect ratio
 ρ density, kg/m³
 μ viscosity, kg/ms
 \emptyset channel angle, radian

Subscripts/Superscripts

i inner
o outer
* non-dimensional

References

- [1] Hartnett JP, Irvine TF (1957) Nusselt values for estimating turbulent liquid metal heat transfer in noncircular ducts. *AIChE J* 3(3): 313–317.
- [2] Barletta A (1996) On forced convection in a circular duct with slug flow and viscous dissipation. *Int Comm Heat Mass Transfer* 23(1): 69–78.
- [3] Barletta A, Zanchini E (1997) Forced convection in the thermal entrance region of a circular duct with slug flow and viscous dissipation. *Int J Heat Mass Transfer* 40(5): 1181–1190.
- [4] Barletta A (1997) Slug flow heat transfer in circular ducts with viscous dissipation and convective boundary conditions. *Int J Heat Mass Transfer* 40(17): 4219–4228.
- [5] Gao SX, Hartnett JP (1993) Analytical Nusselt number predictions for slug flow in rectangular duct. *Int Comm Heat Mass Transfer* 20: 751–760.
- [6] Spiga M, Morini GL (1998) The developing Nusselt numbers for slug flow in rectangular ducts. *Int J Heat Mass Transfer* 41: 2799–2807.
- [7] Morini GL (1999) Thermal characteristics of slug flow in rectangular ducts. *Int J Thermal Sci* 38: 148–159.
- [8] Barletta A, Pulvirenti B (2000) Forced convection with slug flow and viscous dissipation in a rectangular duct. *Int J Heat Mass Transfer* 43: 725–740.
- [9] Muzychka YS, Yovanovich MM (2002) Laminar flow friction and heat transfer in non-circular ducts and channels: part ii- thermal problem. *Proc of Compact Heat Exchangers, A festschrift on the 60th birthday of Ramesh K. Shah, Grenoble, France.*
- [10] Thiart GD (1990) Exact solution for slug flow laminar heat transfer development in a rectangular duct with isothermal walls. *ASME J Heat Transfer* 112: 499–501.
- [11] Nield DA, Lage JL (1998) The role of longitudinal diffusion in fully developed forced convective slug flow in a channel. *Int J Heat Mass Transfer* 41: 4375–4377.
- [12] Shah RK, London AL (1978) *Laminar flow forced convection in ducts.* Academic press, New York.
- [13] Bahrami M, Yovanovich MM, Culham JR (2007) A novel solution for pressure drop in singly connected microchannels of arbitrary cross-section. *Int J Heat Mass Transfer* 50: 2492–2502.
- [14] Asako Y, Nakamura H, Faghri M (1998) Developing laminar flow and heat transfer in the entrance region of regular polygonal ducts. *Int J Heat Mass Transfer* 31(12): 2590–2593.
- [15] Shah RK, Bhatti MS (1987) Laminar convective heat transfer in ducts. in: Kakac S, Shah RK, Aung W (eds.), *Handbook of Single-phase Convective Heat Transfer*, Wiley, New York.